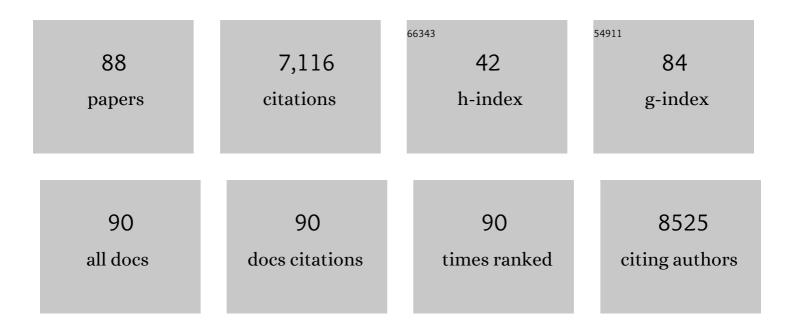
List of Publications by Year in descending order

Source: https://exaly.com/author-pdf/4782149/publications.pdf Version: 2024-02-01



TAKESHI MODIKANAA

#	Article	IF	CITATIONS
1	A Highly Durable, Self-Photosensitized Mononuclear Ruthenium Catalyst for CO2 Reduction. Synlett, 2022, 33, 1137-1141.	1.8	8
2	Photocatalytic CO ₂ Reduction Using Water as an Electron Donor under Visible Light Irradiation by Z-Scheme and Photoelectrochemical Systems over (CuGa) _{0.5} ZnS ₂ in the Presence of Basic Additives. Journal of the American Chemical Society, 2022, 144, 2323-2332.	13.7	56
3	Hot-carrier photocatalysts for artificial photosynthesis. Journal of Chemical Physics, 2022, 156, 164705.	3.0	1
4	Solar-Driven CO ₂ Reduction Using a Semiconductor/Molecule Hybrid Photosystem: From Photocatalysts to a Monolithic Artificial Leaf. Accounts of Chemical Research, 2022, 55, 933-943.	15.6	47
5	Photocatalytic CO ₂ Reduction Using an Iron–Bipyridyl Complex Supported by Two Phosphines for Improving Catalyst Durability. Organometallics, 2022, 41, 1865-1871.	2.3	7
6	Photocatalytic CO2 reduction by a Z-scheme mechanism in an aqueous suspension of particulate (CuGa)0.3Zn1.4S2, BiVO4 and a Co complex operating dual-functionally as an electron mediator and as a cocatalyst. Applied Catalysis B: Environmental, 2022, 316, 121600.	20.2	8
7	Study of Excited States and Electron Transfer of Semiconductorâ€Metalâ€Complex Hybrid Photocatalysts for CO 2 Reduction by Using Picosecond Timeâ€Resolved Spectroscopies. Chemistry - A European Journal, 2021, 27, 1127-1137.	3.3	4
8	A large-sized cell for solar-driven CO2 conversion with a solar-to-formate conversion efficiency of 7.2%. Joule, 2021, 5, 687-705.	24.0	54
9	Carbon Nanohorn Support for Solar driven CO ₂ Reduction to CO Catalyzed by Mnâ€complex in an All Earthâ€abundant System. ChemNanoMat, 2021, 7, 596-599.	2.8	3
10	Electrochemical CO ₂ Reduction to HCOOH Catalyzed by Ag <i>_n</i> (NO ₃) <i>_n</i> ₊₁ Clusters Prepared by Laser Ablation at the Air-Liquid Interface. Chemistry Letters, 2021, 50, 1941-1944.	1.3	0
11	Electrochemical CO2 reduction improved by tuning the Cu-Cu distance in halogen-bridged dinuclear cuprous coordination polymers. Journal of Catalysis, 2021, 404, 12-17.	6.2	5
12	Particulate photocatalytic reactors with spectrum-splitting function for artificial photosynthesis. Physical Chemistry Chemical Physics, 2021, 23, 15659-15674.	2.8	2
13	Solar Fuel Production from CO ₂ Using a 1 m-Square-Sized Reactor with a Solar-to-Formate Conversion Efficiency of 10.5%. ACS Sustainable Chemistry and Engineering, 2021, 9, 16031-16037.	6.7	18
14	Photoelectrochemical water-splitting over a surface modified p-type Cr ₂ O ₃ photocathode. Dalton Transactions, 2020, 49, 659-666.	3.3	23
15	Charge Trapping Process in Photoexcited Nitrogen-Doped Titanium Oxides. Inorganic Chemistry, 2020, 59, 10439-10449.	4.0	3
16	Electrochemical CO ₂ reduction over nanoparticles derived from an oxidized Cu–Ni intermetallic alloy. Chemical Communications, 2020, 56, 15008-15011.	4.1	10
17	Low-Overpotential Electrochemical Water Oxidation Catalyzed by CuO Derived from 2 nm-Sized Cu ₂ (NO ₃)(OH) ₃ Nanoparticles Generated by Laser Ablation at the Air–Liquid Interface. ACS Applied Energy Materials, 2020, 3, 8383-8392.	5.1	12
18	Self-assembled Cuprous Coordination Polymer as a Catalyst for CO ₂ Electrochemical Reduction into C ₂ Products. ACS Catalysis, 2020, 10, 10412-10419.	11.2	44

#	Article	IF	CITATIONS
19	Photocatalytic CO ₂ Reduction Using a Robust Multifunctional Iridium Complex toward the Selective Formation of Formic Acid. Journal of the American Chemical Society, 2020, 142, 10261-10266.	13.7	90
20	Formation of C2 organic molecules from CO ₂ and H ₂ O by femtosecond laser induced chemical reactions in water. Japanese Journal of Applied Physics, 2020, 59, 057001.	1.5	4
21	Spectrally robust series/parallel-connected triple-junction photovoltaic cells used for artificial photosynthesis. Journal of Applied Physics, 2020, 127, .	2.5	8
22	Operando X-ray absorption spectroscopy of hyperfine β-FeOOH nanorods modified with amorphous Ni(OH)2 under electrocatalytic water oxidation conditions. Chemical Communications, 2020, 56, 5158-5161.	4.1	12
23	High-pressure synthesis of ε-FeOOH from β-FeOOH and its application to the water oxidation catalyst. RSC Advances, 2020, 10, 44756-44767.	3.6	6
24	Solar-driven CO ₂ to CO reduction utilizing H ₂ O as an electron donor by earth-abundant Mn–bipyridine complex and Ni-modified Fe-oxyhydroxide catalysts activated in a single-compartment reactor. Chemical Communications, 2019, 55, 237-240.	4.1	33
25	First principles calculations of surface dependent electronic structures: a study on β-FeOOH and γ-FeOOH. Physical Chemistry Chemical Physics, 2019, 21, 18486-18494.	2.8	17
26	Molecular Catalysts Immobilized on Semiconductor Photosensitizers for Proton Reduction toward Visible‣ightâ€Driven Overall Water Splitting. ChemSusChem, 2019, 12, 1807-1824.	6.8	25
27	Self-Assembled Single-Crystalline GaN Having a Bimodal Meso/Macropore Structure To Enhance Photoabsorption and Photocatalytic Reactions. ACS Applied Materials & Interfaces, 2019, 11, 4233-4241.	8.0	11
28	Highly Enhanced Electrochemical Water Oxidation Reaction over Hyperfine β-FeOOH(Cl):Ni Nanorod Electrode by Modification with Amorphous Ni(OH)2. Bulletin of the Chemical Society of Japan, 2018, 91, 778-786.	3.2	24
29	Low-Energy Electrocatalytic CO ₂ Reduction in Water over Mn-Complex Catalyst Electrode Aided by a Nanocarbon Support and K ⁺ Cations. ACS Catalysis, 2018, 8, 4452-4458.	11.2	79
30	Band bending and dipole effect at interface of metal-nanoparticles and TiO ₂ directly observed by angular-resolved hard X-ray photoemission spectroscopy. Physical Chemistry Chemical Physics, 2018, 20, 11342-11346.	2.8	12
31	Effects of Ta ₂ O ₅ Surface Modification by NH ₃ on the Electronic Structure of a Ru-Complex/N–Ta ₂ O ₅ Hybrid Photocatalyst for Selective CO ₂ Reduction. Journal of Physical Chemistry C, 2018, 122, 1921-1929.	3.1	12
32	Solar-Driven Photocatalytic CO ₂ Reduction in Water Utilizing a Ruthenium Complex Catalyst on p-Type Fe ₂ O ₃ with a Multiheterojunction. ACS Catalysis, 2018, 8, 1405-1416.	11.2	110
33	Light-Driven Carbon Dioxide Reduction Devices. Green Chemistry and Sustainable Technology, 2018, , 259-280.	0.7	2
34	Sodium hexatitanate photocatalysts prepared by a flux method for reduction of carbon dioxide with water. Catalysis Today, 2018, 303, 296-304.	4.4	26
35	[Ir(tpy)(bpy)Cl] as a Photocatalyst for CO ₂ Reduction under Visible‣ight Irradiation. ChemPhotoChem, 2018, 2, 207-212.	3.0	32
36	Electrocatalytic CO ₂ reduction near the theoretical potential in water using Ru complex supported on carbon nanotubes. Nanotechnology, 2018, 29, 034001.	2.6	19

#	Article	IF	CITATIONS
37	Enhancement of CO2 reduction activity under visible light irradiation over Zn-based metal sulfides by combination with Ru-complex catalysts. Applied Catalysis B: Environmental, 2018, 224, 572-578.	20.2	55
38	Electrochemical Water Oxidation Catalysed by CoOâ€Co ₂ O ₃ â€Co(OH) ₂ Multiphaseâ€Nanoparticles Prepared by Femtosecond Laser Ablation in Water. ChemistrySelect, 2018, 3, 4979-4984.	1.5	14
39	Z-Schematic and visible-light-driven CO ₂ reduction using H ₂ O as an electron donor by a particulate mixture of a Ru-complex/(CuGa) _{1â^²x} Zn _{2x} S ₂ hybrid catalyst, BiVO ₄ and an electron mediator. Chemical Communications, 2018, 54, 10199-10202.	4.1	52
40	Highly crystalline β-FeOOH(Cl) nanorod catalysts doped with transition metals for efficient water oxidation. Sustainable Energy and Fuels, 2017, 1, 636-643.	4.9	40
41	Stoichiometric water splitting using a p-type Fe ₂ O ₃ based photocathode with the aid of a multi-heterojunction. Journal of Materials Chemistry A, 2017, 5, 6483-6493.	10.3	34
42	Photoelectrochemical hydrogen production by water splitting over dual-functionally modified oxide: p-Type N-doped Ta2O5 photocathode active under visible light irradiation. Applied Catalysis B: Environmental, 2017, 202, 597-604.	20.2	49
43	Evaluation of photocatalytic activities and characteristics of Cu- or Fe-modified nitrogen-doped titanium dioxides for applications in environmental purification. Japanese Journal of Applied Physics, 2016, 55, 01AA05.	1.5	10
44	Carbon microfiber layer as noble metal-catalyst support for selective CO2 photoconversion in phosphate solution: Toward artificial photosynthesis in a single-compartment reactor. Journal of Photochemistry and Photobiology A: Chemistry, 2016, 327, 1-5.	3.9	8
45	Aminoalkylsilane-modified Silver Cathodes for Electrochemical CO ₂ Reduction. Chemistry Letters, 2016, 45, 1362-1364.	1.3	3
46	CO2 Reduction by Photoelectrochemistry. Lecture Notes in Energy, 2016, , 281-296.	0.3	4
47	Photoelectrochemical CO ₂ reduction using a Ru(<scp>ii</scp>)–Re(<scp>i</scp>) multinuclear metal complex on a p-type semiconducting NiO electrode. Chemical Communications, 2015, 51, 10722-10725.	4.1	131
48	A monolithic device for CO ₂ photoreduction to generate liquid organic substances in a single-compartment reactor. Energy and Environmental Science, 2015, 8, 1998-2002.	30.8	157
49	Z-scheme water splitting under visible light irradiation over powdered metal-complex/semiconductor hybrid photocatalysts mediated by reduced graphene oxide. Journal of Materials Chemistry A, 2015, 3, 13283-13290.	10.3	65
50	Toward Solar-Driven Photocatalytic CO ₂ Reduction Using Water as an Electron Donor. Inorganic Chemistry, 2015, 54, 5105-5113.	4.0	115
51	Nitrogen-Doped Titanium Dioxide as Visible-Light-Sensitive Photocatalyst: Designs, Developments, and Prospects. Chemical Reviews, 2014, 114, 9824-9852.	47.7	1,086
52	Structural Improvement of CaFe ₂ O ₄ by Metal Doping toward Enhanced Cathodic Photocurrent. ACS Applied Materials & Interfaces, 2014, 6, 10969-10973.	8.0	65
53	Nitrogen and transition-metal codoped titania nanotube arrays for visible-light-sensitive photoelectrochemical water oxidation. Chemical Communications, 2014, 50, 7614.	4.1	17
54	Charge-Carrier Dynamics in Cu- or Fe-Loaded Nitrogen-Doped TiO ₂ Powder Studied by Femtosecond Diffuse Reflectance Spectroscopy. Journal of Physical Chemistry C, 2013, 117, 16448-16456.	3.1	42

#	Article	IF	CITATIONS
55	A Highly Efficient Mononuclear Iridium Complex Photocatalyst for CO ₂ Reduction under Visible Light. Angewandte Chemie - International Edition, 2013, 52, 988-992.	13.8	277
56	Solar CO2 reduction using H2O by a semiconductor/metal-complex hybrid photocatalyst: enhanced efficiency and demonstration of a wireless system using SrTiO3 photoanodes. Energy and Environmental Science, 2013, 6, 1274.	30.8	251
57	Photoactivity of p-Type α-Fe ₂ O ₃ Induced by Anionic/Cationic Codoping of N and Zn. Applied Physics Express, 2013, 6, 041201.	2.4	14
58	Charge-Carrier Dynamics in Nitrogen-Doped TiO ₂ Powder Studied by Femtosecond Time-Resolved Diffuse Reflectance Spectroscopy. Journal of Physical Chemistry C, 2012, 116, 1286-1292.	3.1	58
59	Visible light-sensitive mesoporous N-doped Ta2O5 spheres: synthesis and photocatalytic activity for hydrogen evolution and CO2 reduction. Journal of Materials Chemistry, 2012, 22, 24584.	6.7	65
60	Photoinduced Electron Transfer from Nitrogen-Doped Tantalum Oxide to Adsorbed Ruthenium Complex. Journal of Physical Chemistry C, 2011, 115, 18348-18353.	3.1	58
61	Selective CO2 conversion to formate in water using a CZTS photocathode modified with a ruthenium complex polymer. Chemical Communications, 2011, 47, 12664.	4.1	127
62	Direct assembly synthesis of metal complex–semiconductor hybrid photocatalysts anchored by phosphonate for highly efficient CO2 reduction. Chemical Communications, 2011, 47, 8673.	4.1	108
63	p -type conduction induced by N-doping in \hat{I}_{\pm} -Fe2O3. Applied Physics Letters, 2011, 98, .	3.3	37
64	Selective CO ₂ Conversion to Formate Conjugated with H ₂ O Oxidation Utilizing Semiconductor/Complex Hybrid Photocatalysts. Journal of the American Chemical Society, 2011, 133, 15240-15243.	13.7	458
65	Visibleâ€Lightâ€Induced Selective CO ₂ Reduction Utilizing a Ruthenium Complex Electrocatalyst Linked to a pâ€Type Nitrogenâ€Doped Ta ₂ O ₅ Semiconductor. Angewandte Chemie - International Edition, 2010, 49, 5101-5105.	13.8	325
66	Synthesis and Optical Properties of Monolayer Organosilicon Nanosheets. Journal of the American Chemical Society, 2010, 132, 5946-5947.	13.7	154
67	Dual functional modification by N doping of Ta2O5: p-type conduction in visible-light-activated N-doped Ta2O5. Applied Physics Letters, 2010, 96, .	3.3	56
68	Charge Separation and Trapping in N-Doped TiO ₂ Photocatalysts: A Time-Resolved Microwave Conductivity Study. Journal of Physical Chemistry Letters, 2010, 1, 3261-3265.	4.6	103
69	Photoelectrochemical reduction of CO2 in water under visible-light irradiation by a p-type InP photocathode modified with an electropolymerized ruthenium complex. Chemical Communications, 2010, 46, 6944.	4.1	180
70	Remarkably enhanced photocatalytic activity by nickel nanoparticle deposition on sulfur-doped titanium dioxide thin film. Applied Catalysis B: Environmental, 2009, 87, 239-244.	20.2	37
71	Optical bandgap widening of p-type Cu2O films by nitrogen doping. Applied Physics Letters, 2009, 94, .	3.3	156
72	Visible-light-induced photocatalytic oxidation of carboxylic acids and aldehydes over N-doped TiO2 loaded with Fe, Cu or Pt. Applied Catalysis B: Environmental, 2008, 83, 56-62.	20.2	110

#	Article	IF	CITATIONS
73	Photocatalytic Oxidation of NOx under Visible LED Light Irradiation over Nitrogen-Doped Titania Particles with Iron or Platinum Loading. Journal of Physical Chemistry C, 2008, 112, 12425-12431.	3.1	119
74	Materials design and development of functional materials for industry. Journal of Physics Condensed Matter, 2008, 20, 064227.	1.8	15
75	Emissive Interface States in Organic Light-Emitting Diodes Based on Tris(8-hydroxyquinoline) Aluminum. Japanese Journal of Applied Physics, 2008, 47, 464-467.	1.5	6
76	Deep-Level Characterization of Tris(8-hydroxyquinoline) Aluminum with and without Quinacridone Doping. Japanese Journal of Applied Physics, 2007, 46, 2636-2639.	1.5	6
77	Origin of visible-light sensitivity in N-doped TiO2 films. Chemical Physics, 2007, 339, 20-26.	1.9	58
78	Nitrogen complex species and its chemical nature in TiO2 for visible-light sensitized photocatalysis. Chemical Physics, 2007, 339, 57-63.	1.9	214
79	Electrical characterization of p-type N-doped ZnO films prepared by thermal oxidation of sputtered Zn3N2 films. Applied Physics Letters, 2006, 88, 172103.	3.3	105
80	Trap levels in tris(8-hydroxyquinoline) aluminum studied by deep-level optical spectroscopy. Applied Physics Letters, 2006, 88, 252104.	3.3	8
81	Photodegradation of toluene over TiO2–xNx under visible light irradiation. Physical Chemistry Chemical Physics, 2006, 8, 1116.	2.8	120
82	Photocatalytic Degradation of Formaldehyde and Toluene Mixtures in Air with a Nitrogen-doped TiO2Photocatalyst. Chemistry Letters, 2006, 35, 616-617.	1.3	20
83	Enhanced photocatalytic activity of TiO2â^'xNx loaded with copper ions under visible light irradiation. Applied Catalysis A: General, 2006, 314, 123-127.	4.3	126
84	Deep-Level Optical Spectroscopy Investigation of Trap Levels in Tris(8-Hydroxyquinoline) Aluminum. Materials Research Society Symposia Proceedings, 2006, 965, 1.	0.1	0
85	Deep-level characterization of N-doped ZnO films prepared by reactive magnetron sputtering. Applied Physics Letters, 2005, 87, 232104.	3.3	35
86	Electrical characterization of band gap states in C-doped TiO2 films. Applied Physics Letters, 2005, 87, 052111.	3.3	68
87	Deep-level optical spectroscopy investigation of N-doped TiO2 films. Applied Physics Letters, 2005, 86, 132104.	3.3	191
88	Band-Gap Narrowing of Titanium Dioxide by Nitrogen Doping. Japanese Journal of Applied Physics, 2001, 40, L561-L563.	1.5	541